Desalination and Water Treatment
www.deswater.com

doi: 10.1080/19443994.2016.1162202

57 (2016) 26153–26164
November

Taylor & Francis
Taylor & Francis Group

Removal of phenolic pollutants from aqueous solutions by a simple magnetic separation

Bilsen Tural*, Erdal Ertaş, Servet Tural

Faculty of Education, Department of Chemistry, Dicle University, Diyarbakir 21280, Turkey, Tel. +90 412 2488030, ext. 8915; Fax: +90 412 2488257; emails: bilsentural@gmail.com (B. Tural), erdalertas21@gmail.com (E. Ertaş), servet.tural@hotmail.com (S. Tural)

Received 5 November 2015; Accepted 1 March 2016

ABSTRACT

The removal efficiencies of phenol, 2-chlorophenol (2-CPh), and 4-chlorophenol (4-CPh) from aqueous solution with magnetic chitosan nanoparticles were investigated in this work. Chitosan-coated magnetite nanoparticles were successfully synthesized, characterizated, and applied as an effective magnetic biosorbent for the removal of phenol, 2-CPh, and 4-CPh from aqueous solutions. The characterization of synthesized magnetic chitosan nanoparticles was performed by Fourier transform infrared spectroscopy, transmission electron microscopy, scanning electron microscopy, dynamic light scattering, vibrating sample magnetometry analyses, and thermogravimetric analysis. Adsorption characteristics of phenolic compounds from aqueous solution on to magnetic chitosan have been studied and results indicated that the adsorption capacities were affected by initial pH values, initial concentration of adsorbates, dosage of adsorbent, and contact time. The adsorption of adsorbates followed with the pseudo-second-order reaction and equilibrium experiments were well fitted with the Freundlich isotherm model. Furthermore, it was found that the magnetic biosorbent can be regenerated and reused for five repeated cycles for the removal of phenol, 2-CPh, and 4-CPh and avoided secondary pollution of biosorbent to water.

Keywords: Magnetic biosorbent; Phenolic pollutants adsorption; Magnetic separation; Water purification

1. Introduction

Phenol and phenolic compounds are widely used in chemical industrial applications such as pesticides, petroleum rafineries, synthetic rubber, plastic, and petrochemicals [1]. Therefore, they are often released in effluents during processing and transforming and are causing health and environmental problems. Due to their high toxicity and persistence in the environment, both the US Environmental Protection Agency (EPA) and the European Union have selected phenols as priority pollutants [1,2]. Growing concern for public health and environmental quality has caused the establishment of rigid limits on the acceptable environmental levels of specific pollutants [2]. Therefore, keeping the hazardous effects of phenolic compounds in view, attempts have been made by various researchers to remove phenolic compounds from wastewater [3–5].

The customary methods, for instance ion exchange, adsorption, solvent extraction, microbial degradation, chemical oxidation, precipitation, distillation,

*Corresponding author.

membrane processes, and reverse osmosis, have been substantially applied for removing phenols from aqueous solutions [1,2,6,7]. Among these methods, adsorption has increasingly received more attention due to its merits of effectiveness, efficiency and economy for removing phenolic compounds [3,4,8].

A number of adsorption materials have been used to remove phenolic compounds including ion exchange resins, crushed coals, straws, and activated carbon [9–11]. Generally, their effectiveness increases with a decrease of the particle size. However, solid/liquid (S/L) separation is more difficult as the particle size decreases. Therefore, efforts are still required to carry out investigation for new separation techniques.

In recent years, there has been increased interest in the use of magnetic-assisted separation technique (MAT) which is an alternative to centrifugation or filtration separation methods based on the use of magnetic nanoparticles (MNPs) [12]. In MAT, functionalized magnetic nano-adsorbents are dispersed into samples to adsorb target compounds, and then the sorbents are separated rapidly by applying an external magnetic field. The special advantages of MAT are the fast and simple handling of a sample and the opportunity to deal with large sample volumes without the need for time-consuming centrifugation and filtration steps [13].

Synthesis of MNPs with polymer coating has the potential to control the mean particle size and size distribution of the nanoparticles [14–17]. The polymer layer prevents magnetite nanoparticles from oxidation toward a lower saturation magnetization iron oxide phases [18]. At the same time it creates a platform as adsorbent for application.

Chitosan is a polymer of deacetylation process of chitin, which has increasingly been applied in medicine, pharmacology, biotechnology, as well as plant or environment protection [19]. It is acknowledged as an easily available and inexpensive sorbent. Owing to the fact that it possesses highly reactive amino groups and secondary hydroxyl functional groups as well as the property of nontoxicity and biodegradability, it is characterized by a high adsorption effectiveness of inorganic and organic substances from aqueous solutions [20].

The chitosan is defined as an appropriate natural polymer for adsorption of phenolic compounds [21–25]. The maximum adsorption capacities of phenolic compounds onto unmodified chitosan conducted by various research groups are presented in Table 1 together with the values obtained in the present study [23–36].

In this study, magnetic chitosan nanoparticles (MCNs) were prepared, characterizated and applied as an effective sorbent to remove phenolic compounds from waste water. In addition, the adsorption characteristics of phenolic compounds from aqueous solutions on MCNs were investigated. The kinetic of phenol, 2-chlorophenol (2-CPh), and 4-chlorophenol (4-CPh) adsorption onto MCNs was investigated by the pseudo-first-order and pseudo-second-order models and the equilibrium data were analyzed by the Langmuir and Freundlich isotherms using the linear regression analysis. To the best of our knowledge, despite the chitosan and its derivatives have been used to remove phenolic compounds from aqueous solutions, their use as magnetic nano-biomaterial has not yet been studied for this purpose.

2. Materials and methods

2.1. Chemicals and reagents

$FeCl_3{\cdot}6H_2O$, $FeCl_2{\cdot}4H_2O$, NaOH beads (95–100%), HCl (36.5–38%), ammonium hydroxide solution (26% NH_3), phenol, 2-CPh, and 4-CPh were obtained by Sigma-Aldrich. Chitosan powder with molecular weight of 10,000–30,000 and degree of deacetylation of >75% was obtained from Sigma-Aldrich. About 99% pure oxalic acid dihydrate was obtained by Merck.

A known amount of phenol, 2-CPh, and 4-CPh were taken and soluted dissolved in a 1,000 mL of distiled water for preparing stock solutions. Desired concentrations of phenols were prepared from an aqueous phenols stock solutions by suitably diluting with distilled water.

2.2. Characterization

MCNs were redispersed in pure water by sonication for 10 s. The particles were redispersed in distilled-deionized water by sonication for 10 s and a drop of suspension was placed onto SPI Double Copper Grids 100/200. Quanta 400F field emission scanning electron microscopy (FE-SEM (FEI)) was used for morphological characterization of the MCNs. The particles were analyzed by transmission electron microscopy (TEM) (JEOL 2100F, Japan) for particle size and morphology. Fourier transformed infrared (FT-IR) spectra were measured on a Thermo Scientific Nicolet IS10 FT-IR spectrometer (USA). Sixteen scans were collected at a resolution of 4 cm^{-1}. The particle agglomeration size distributions of the MNPs and MCNs were measured using a laser particle sizer (Mastersizer 2000, Malvern, England). Magnetization measurements were conducted using a cryogenic magnetometer (Quantum Design PPMS-9T) in the room temperature. Thermogravimetric analysis (TGA) and differential

Table 1
Maximum capacity, Q^0 (mg/g), for adsorption of phenolic compounds by chitosan

Sorbent	Adsorbates, Q^0 (mg/g)			Refs.
	phenol	2-CP	4-CP	
CS/Ab blended beads	156	204	278	[23]
Chitosan[a]	1.26			[24]
Chitosan-coated perlite beads	192	263	322	[25]
Chitosan[a] (CS)	2.2		2.6	[26]
CS-SA	8.50		20.49	
CS-CD	34.93		179.73	
EPI-CD	131.50		74.25	
CS/CA blended beads	109	97		[27]
Sugar cane bagasse fly ash	23.83			[28]
Ratan sawdust-based activated carbon	149.25			[29]
Granular activated carbon	165.80			[30]
Commercial activated carbon	49.72			[31]
M-bentonite	9.9			[32]
Al-bentonite	8.7			
CTAB-bentonite	8.4			
T-bentonite	8.2			
CS850A	205.8			[33]
Fly ash	3.85			[34]
Modified bentonite			176.6	[35]
Perlite			5.84	[36]
MCNs[b]	196	244	323	Present study

[a]Unmodified Chitosan.
[b]Magnetic Chitosan.

thermal analysis were performed with a Shimadzu DTG-60 (Japan) at a heating rate of 10°C/min in N_2 atmosphere.

2.3. Preparation of magnetic chitosan nanoparticles

MNPs were prepared by the chemical coprecipitation method as reported in our previous work [37,38]. The chitosan solution was prepared by dissolving 0.75 g of low molecular wieght chitosan in 25 mL of 0.2 M oxalic acid under magnetic stirring 500 rpm. The viscous chitosan solution was mixed for 1 h at 40–50°C. Colloid solution was obtained by the addition of 2.25 g MNPs to 25 mL distiled water. The chitosan solution and MNPs colloid solution were mixed for 16 h at 40–50°C. Then, the magnetic-chitosan gel was added dropwise into a 0.7 M NaOH to assist rapid neutralization of oxalic acid [39]. These MCNs were separated with a magnet from the NaOH bath, and washed several times with deionized water to a neutral pH. The beads are dried in a freeze drier [24].

2.4. Biosorption experiments

Biosorption experiments were carried out batchwise to examine the effect of pH values, contact time, adsorbent dosage, initial adsorbate concentration. The pH is adjusted by dilute aqueous solution of either HCl or NaOH. Experiments were conducted in a set of 25 mL erlenmeyer flasks, where solutions of phenols (50 mL) with different initial concentrations were added in these flasks [29]. In order to ensure the uniform experimental conditions that 30 min is enough to gain equilibrium between sorbent and adsorbate. When reaching equilibrium, the phenols solutions was separated from the adsorbent with a Nd–Fe–B permanent magnet. At predetermined time intervals a definite volume of the supernatant solutions were collected in test tubes. The final concentrations of phenolic compounds were analyzed using a Perkin Elmer UV–vis spectrophotometer at wavelenght of 270 nm for phenol, 274 nm for 2-CPh and 280 nm for 4-CPh.

2.5. Regeneration and reusability of adsorbent

To determine the reusability of MCNs, five cycles of sequential adsorption–desorption were carried out. Each adsorption process was performed in batch mode with 100 mg/L initial concentration of phenolic compounds for 120 min at 30°C. Thereafter, the MCNs were separated from the sample using external magnetic field, and washed lightly with distilled water to

remove the adhered solution. For the desorption process, the collected adsorbent was immersed into 10 mL of NaOH solution at pH 11.0 for 2 h, while it was being rigorously stirred. It is noteworthy that the regenerated adsorbent was washed for several times by deionized water before being entered to the next cycle.

3. Results and discussion

3.1. Characterization of the MCNs

In this study, the magnetization curves of the MNPs and MCNs were obtained by VSM at 25°C (see Fig. 1). As can be seen from the Fig. 1, the saturation magnetization (σs) of the MCNs was about 55.0 emu/g, while the naked MNPs was 66.0 emu/g. The decrease in the saturation magnetization was on account of the increased amount of chitosan integrated in the chitosan-bound magnetic particles. The presence of chitosan on the surface of MNPs decreased the sameness because of quenching of surface moments, resulting in the lessening of magnetic moment in MCNs. A similar decrease in saturation magnetization value was reported by other researchers when MNPs were coated with distinct polymers or modifying agents [40–42].

The TEM image of MCNs in Fig. 2(A) was observed and showed distinct contrasts of MCNs: the dark areas present for crystalline Fe_3O_4 while the bright ones are relevant to chitosan [43]. The particle of sizes were varied from 9 to 13 nm. The particle agglomeration size distributions of the MNPs and MCNs were shown in Fig. 2(B). Z-average particle agglomeration size of the MNPs and the MCNs was determined as 126–762 nm, respectively. These results suggest that the particle agglomeration size of the MNPs was increased significantly (from 126 to 762 nm) when they were coated with chitosan. The observation of surface topography of the MCNs is shown in Fig. 2(C1) and (C2). As can be seen from the SEM image, the surface is rough, porous, folded, and non-hollow.

To confirm the existence of the surface coating, FTIR spectra of the MNPs, the pure chitosan and the MCNs were examined and shown in Fig. 3. For pure chitosan, the peak at 3,287 cm^{-1} is attributed to O–H and N–H stretching vibrations. The C–H stretching vibrations of the polymer backbone is manifested through peaks 2,867 cm^{-1}. The characteristic biosorption peak of primary amine ($–NH_2$) appears at 1,654 cm^{-1} (N–H bending vibrations). The peak at 1,423 cm^{-1} is attributed to C–N stretching vibrations. The biosorption band around 1,020 cm^{-1} displays the

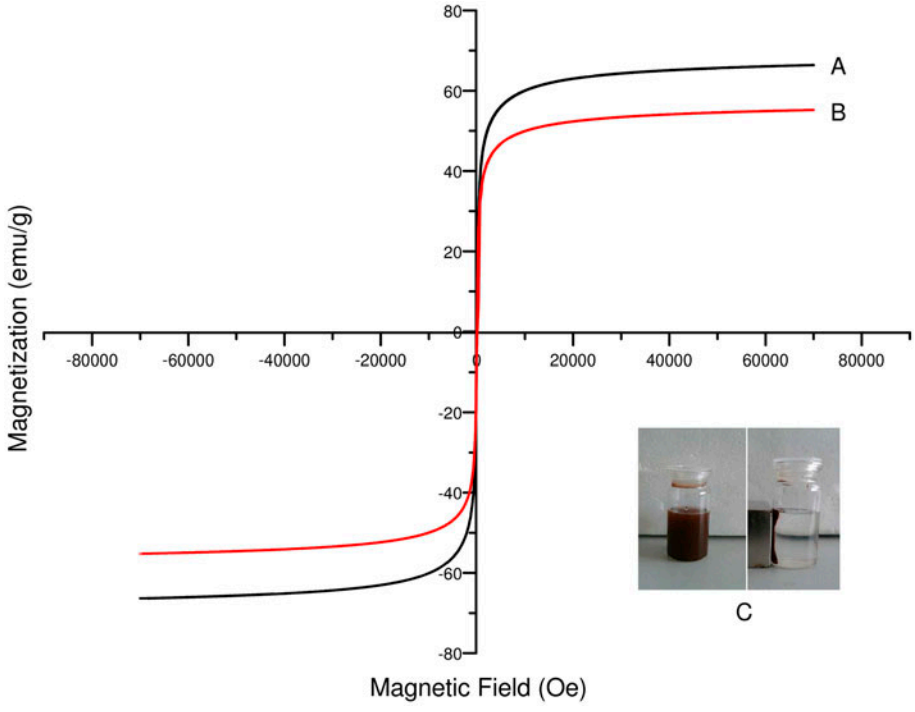

Fig. 1. Magnetization vs. magnetic field for nanoparticles: (A) Fe_3O_4, (B) MCNs, and (C) Response of the magnetic chitosan nanoparticles to the magnetic field.

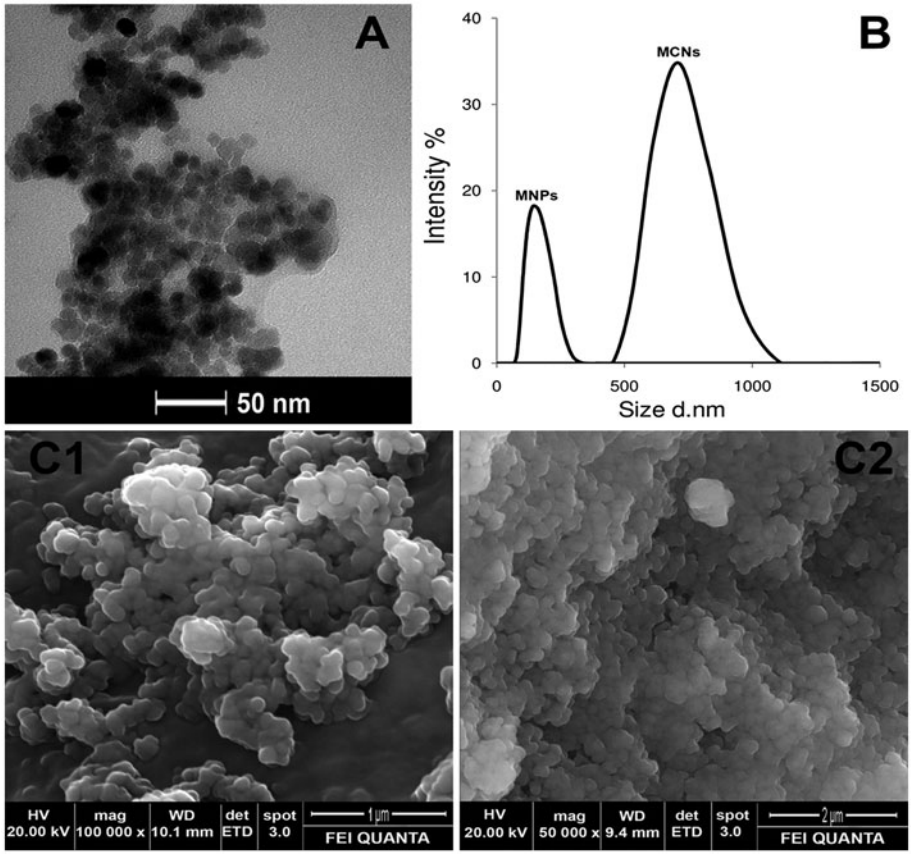

Fig. 2. (A) TEM micrographs for the MCNs, (B) Particle agglomeration size distribution of the naked MNPs and MCNs, and (C) Scanning electron microscopy (SEM) for the MCNs 1. The bars are 1 µm 2. The bars are 2 µm.

stretch vibration of C–O bond. The spectrum of the MCNs shows three characteristic absorption peak for the chitosan (signal at 2,867, 1,640, and 1,032 cm^{-1}) and one additional at 570 cm^{-1}, which corresponds to Fe–O stretching vibrations in magnetite and maghemite. The FT-IR spectra indicated that chitosan is presented in MNPs, and the MNPs were coated by the chitosan [43,44].

The TGA of the chitosan, MNPs and MCNs are shown in Fig. 4. The TGA curve shows that the weight loss of MNPs over the temperature range from 25 to 200˚C is about 1.5% which is attributed to the loss of residual water. On the other hand, the weight loss of MCNs below 200˚C is about 4.8% because of the removal of absorbed physical and chemical water. When the temperature was raised from 200 to 550˚C, the weight loss is significant and about 21% because chitosan was degraded. There was no significant weight change from 550 to 800˚C, implying the presence of only iron oxide within the temperature range [40]. As can be seen from the Fig. 4, the weight loss of chitosan below 200˚C was attributed to the release of water molecules. The decomposition of chitosan starts about 200˚C. The overall weight loss was 69% up to 800˚C [45].

3.2. Effect of pH value

The biosorption of phenol, 2-CPh, and 4-CPh were carried out in the pH range of 5.0–11.0. The biosorption experiments with pH were conducted at an initial phenol, 2-CPh, and 4-CPh concentration of 50 mg/L, 50 mg MCNs, and 200 rpm stirring rate for 30 min at 30˚C. The pH on the biosorption of phenol, 2-CPh, and 4-CPh is shown in Fig. 5. As it can be seen from the Fig. 5, with increasing pH, the removal efficiencies of the phenol, 2-CPh, and 4-CPh does not change obviously at first, but decreases sharply after pH 7.0. According to previous reports [25,46,47] pK_a of phenol, 2-CPh, and 4-CPh was reported as 9.9, 8.3, and 9.2, respectively. When the pH of a solutions goes beyond the pK_a, phenols mainly exist as negative phenolate ions, whereas they exist as molecular form below the pK_a. Due to the negative charges on the

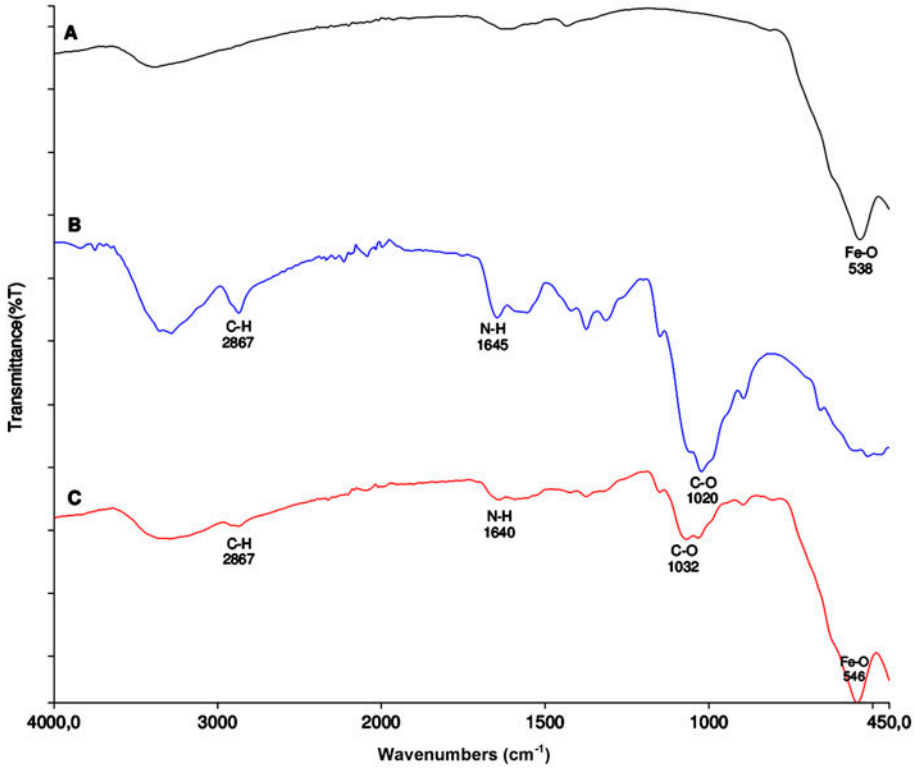

Fig. 3. FTIR spectra of samples: (A) the naked Fe_3O_4, (B) Chitosan, and (C) MCNs.

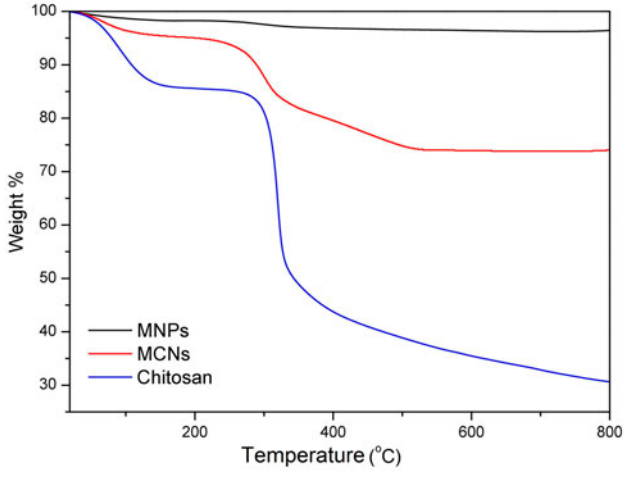

Fig. 4. TGA of the MNPs, MCNs and Chitosan.

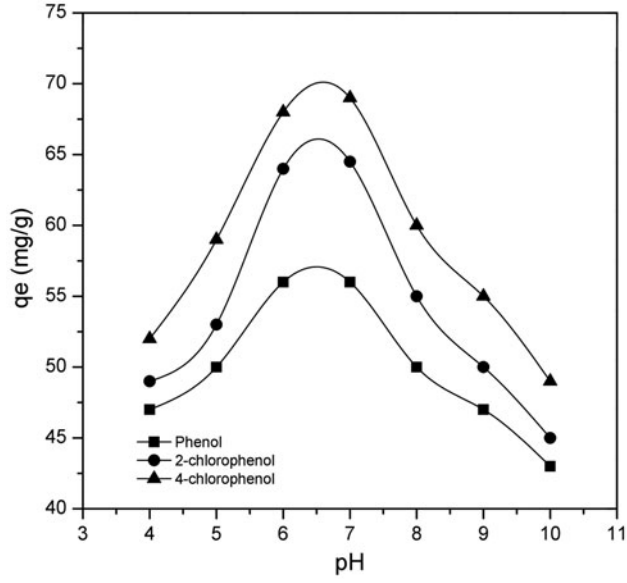

Fig. 5. Effect of pH on biosorption of phenol, 2-CPh, and 4-CPh on MCNs.

phenolate ions, the presence of hydroxyl ions on the adsorbent prevents the binding of phenolate ions that leads to low adsorption of phenolic compounds. Therefore, we consider that phenols effectively adsorbed onto adsorbent are molecules not phenolate anions. Thus, the molecular interactions including hydrogen bonding, hydrophobic interaction and van der Waals forces are the possible factors for the adsorption of phenols [24,26,46,47].

3.3. Agitation period

Fig. 6(A), (B), and (C) shows the effect of agitation time on the extent of biosorption of phenol, 2-CPh, and 4-CPh on MCNs for different initial concentrations. It can be seen that each of the phenolic compounds biosorption onto MCNs is fast in the first 20 min and then it becomes slower near the equilibrium. The biosorption remains continuous after 30 min, implying that equilibrium has been reached. This can be explained by the large number of available vacant sites on the MCNs surfaces which are gradually occupied in time as a result of biosorption process [27,48]. The biosorption order is 4-CPh > 2-CPh > phenol.

3.4. Adsorbent dose

The effect of adsorbent dose on the biosorption of the phenolic compounds is demonstrated in Fig. 7(A), (B), and (C). From this figure it is evident that percent removal of phenol, 2-CPh, and 4-CPh increases with the increase in adsorbent dose while the adsorption capacity, q_e (mg/g), at equilibrium decreases. This can be attributed to the increased adsorbent surface area and availability of more adsorption sites of adsorbent. It is apparent that the uptake of solute markedly increased up to an adsorbent dose of 50 mg and thereafter no significant increase was observed. Hence, the optimum removal of phenol, 2-CPh, and 4-CPh can be obtained by using 50 mg of biosorbent. The maximum percentage removal for phenol, 2-CPh, and 4-CPh is ~67, ~74, and ~80%, respectively, at equilibrium after 30 min of agitation.

The maximum adsorption capacities of phenolic compounds onto modified and unmodified chitosan conducted by various research groups were compared to the values obtained in the present study in Table 1 [23–36]. High values of sorption capacity obtained for MCNs can be explained by its high surface area to volume ratio and high active surface sites.

3.5. Biosorption isotherm

The equilibrium isotherms are used to describe the adsorbate-adsorbent interactions, and their knowledge is important for both a theoretical and a practical point of view. Various isotherm models have been published in the literature to express experimental data adsorption isotherms. In the present study, Langmuir, Freundlich, and Dubinin–Radushkevich isotherms were employed.

The basic assumption of Langmuir isotherm is based on monolayer coverage of the adsorbate on the homogeneous surface of the biosorbent [49,50]. The linear form of the Langmuir isotherm equation is expressed as (Eq. (1)) [29]:

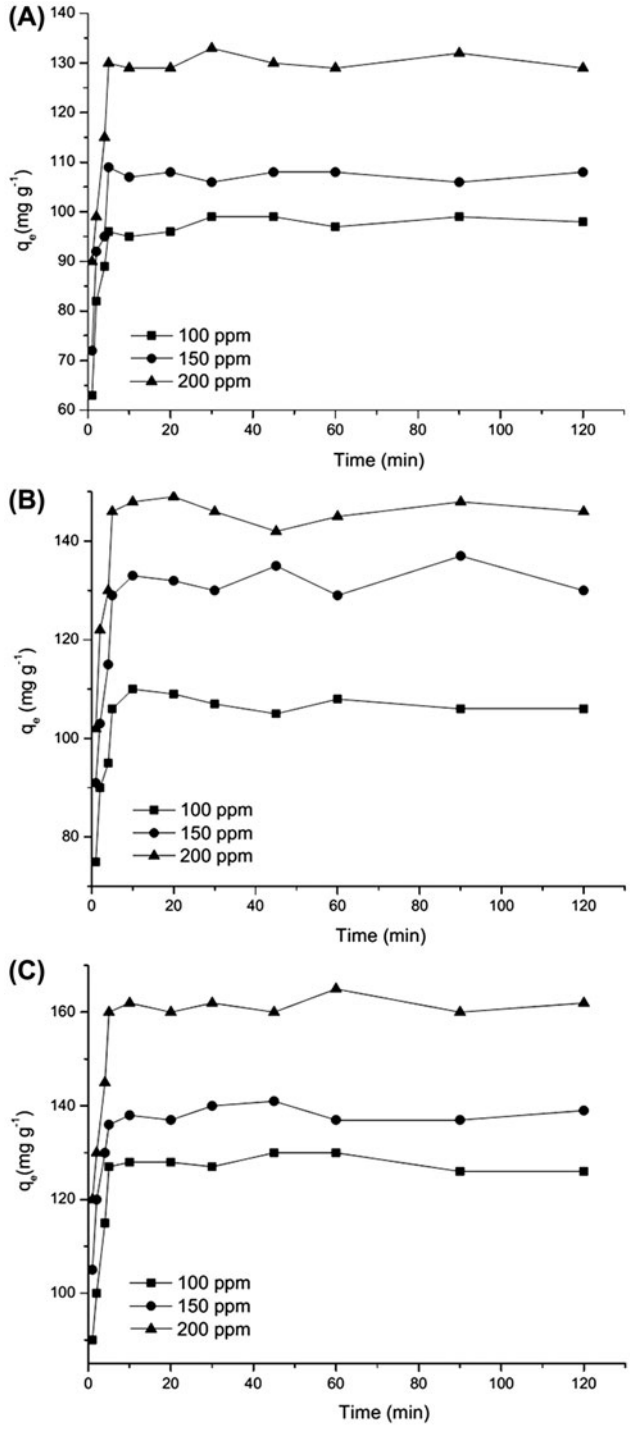

Fig. 6. Effect of agitation time on biosorption of (A) phenol, (B) 2-CPh, and (C) 4-CPh on MCNs at 100, 150, and 200 mg/L initial concentrations.

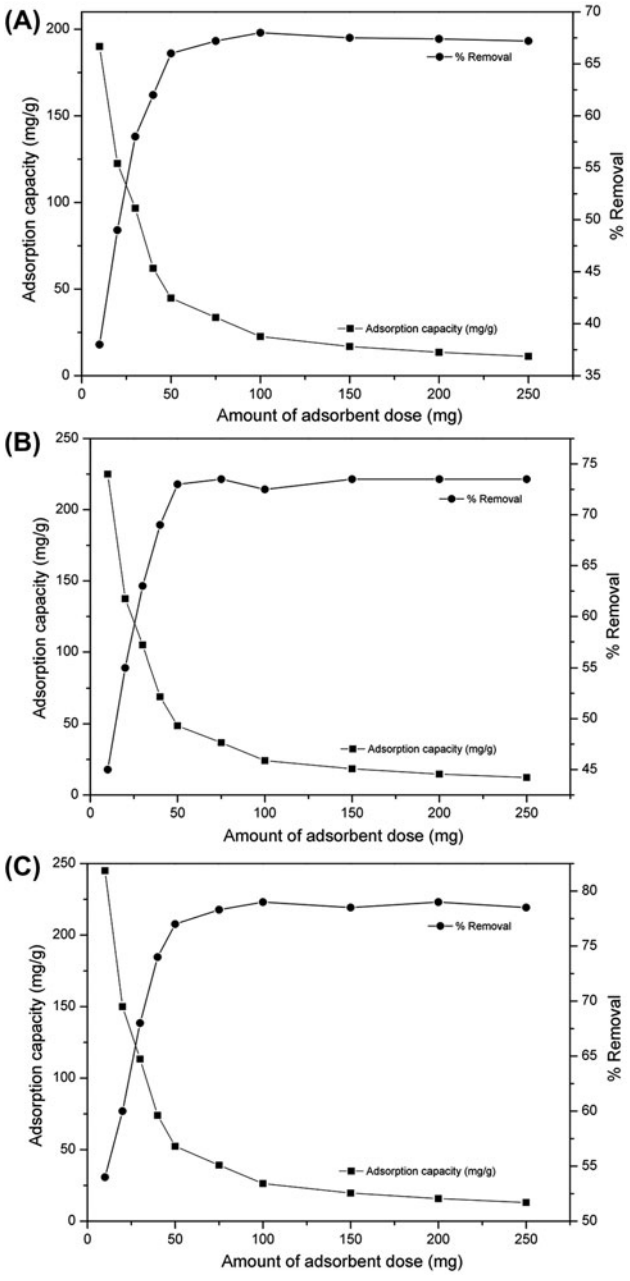

Fig. 7. Effect of adsorbent dose for adsorption of phenolic compounds on MCNs: (A) percent removal of phenol and adsorption capacity (mg/g), (B) percent removal of 2-CPh and adsorption capacity (mg/g), and (C) percent removal of 4-CPh and adsorption capacity (mg/g).

$$\frac{1}{q_e} = \frac{1}{Q_m} + \frac{1}{Q_m K_L} \cdot \frac{1}{C_e} \quad (1)$$

where C_e is the equilibrium concentration of adsorbate (mg/L), q_e (mg/g) is the amount of phenolic compounds adsorbed per unit mass of adsorbent, Q_m the maximum biosorption capacity (mg/g), and K_L is the constant associated with the free energy of adsorption (L/mg). Where Q_m and K_L can be determined from the linear plot of $1/q_e$ vs. $1/C_e$ (see Table 2).

The Freundlich isotherm model used to describe the adsorption characteristics for the heterogeneous adsorbent surface with sites that have diverse energies of adsorption. Hence, the Freundlich equation can be written as the logarithmic form (Eq. (2)) [51]:

$$\text{Log } q_e = \text{Log } K_F + \frac{1}{n} \text{ Log } C_e \quad (2)$$

where q_e is solid phase sorbate concentration in equilibrium (mg/g) and C_e is liquid phase sorbate concentration in equilibrium (mg/L). The constant K_F ($mg^{1-(1/n)} L^{1/n} g^{-1}$) is an approximate indicator of adsorption capacity, while $1/n$ is a function of the strength of adsorption in the adsorption process. The values of K_F and n were obtained by plotting Log (q_e) vs. Log (C_e) and given in Table 2. The n value shows the degree of non-linearity between solution concentration and adsorption as follows: if $n = 1$, then adsorption becomes linear; if $n < 1$, then adsorption becomes a chemical process; if $n > 1$, then adsorption becomes a physical process [52]. In the present study, since n lies between 1.76 and 2.07 (Table 2), the adsorption of phenol, 2-CPh, and 4-CPh on MCNs is a physical process [53].

Langmuir and Freundlich adsorption constants and correlation coefficients (R^2) are presented in Table 2. In both cases, linear plots were gained, which reveal the applicability of these isotherms on the ongoing adsorption process. Results revealed that Freundlich adsorption isotherm was a more linear model than Langmuir for the phenol, 2-CPh, and 4-CPh biosorption on MCNs because correlation Freundlich coefficients (R^2) are greater than Langmuir. The important features of Langmuir adsorption isotherm parameter can be used to foresee the affinity between the sorbates and biosorbent using a dimensionless constant called separation factor or equilibrium parameter (R_L), which is expressed by the following relationship (Eq. (3)) [25,29]:

$$R_L = \frac{1}{1 + bC_0} \quad (3)$$

where b (L/mg) is the Langmuir constant and C_0 (mg/L) is the initial concentration. The value of R_L indicated the type of Langmuir isotherm to be irreversible ($R_L = 0$), linear ($R_L = 1$), unfavorable ($R_L > 1$), or favorable ($0 < R_L < 1$) [54]. The R_L values between 0

Table 2
Isotherms parameters for the adsorption of phenol, 2-CPh, and 4-CPh

	Langmuir isotherm			Freundlich isotherm			Dubinin–Radushkevich isotherm			
Adsorbates	Q_m (mg/g)	K_L (L/mg)	R^2	K_f (L/g)	n	R^2	β (mol^2/kJ)	q_{max} (mg/g)	E (kJ/mol)	R^2
Phenol	196	0.027	0.878	6.97	1.43	0.908	2E-05	165	0.158	0.498
2-chlorophenol	244	0.035	0.904	11.71	1.52	0.940	9E-06	199	0.236	0.540
4-chlorophenol	323	0.038	0.968	18.58	1.64	0.971	6E-06	239	0.289	0.656

and 1 indicate favorable adsorption. The R_L value in the present investigation was found to be 0.1–0.7, indicating that the adsorption of the phenolic compounds on MCNs is favorable.

Dubinin–Radushkevich (D–R) isotherm was also applied to estimate the porosity apparent free energy and the characteristics of adsorption [55–57]. It can be used to describe adsorption on both homogenous and heterogeneous surfaces. The D–R equation can be defined by the following equation (Eq. (4)) [57,58]:

$$\ln q_e = \ln q_{max} - \beta\varepsilon^2 \tag{4}$$

where q_{max} the theoretical saturation capacity, β is a constant related to the adsorption energy, ε the Polanyi potential (mol^2/J^2), calculated from Eq. (5):

$$\varepsilon = RT \ln\left[1 + \frac{1}{C_e}\right] \tag{5}$$

where T is the solution temperature (K), R is the gas constant (8.314 J/mol/K), and C_e is the equilibrium concentration of adsorbate (mg/L). By plotting ln q_e vs. ε^2, it is possible to determine the value of β from the slope and the value of q_{max} (mg/g) from the intercept, which is ln q_{max}. The value of mean free sorption energy, E (kJ/mol), can be estimated by using B values as expressed in the following equation from D–R parameter B as follows (Eq. (6)) [59]:

$$E = \frac{1}{\sqrt{2B}} \tag{6}$$

The extent of E is useful for guessing the type of sorption reaction. If E is in the range of 8–16 kJ/mol, sorption is ruled by chemical ion-exchange. In the case of $E < 8$ kJ/mol, physical forces may affect the biosorption [60]. The parameters obtained using above Eqs. (5) and (6) were evaluated in Table 2. The values calculated using Eq. (6) is 0.224, 0.290, and 0.410 kJ/mol for the phenol, 2-CPh, and 4-CPh, respectively. This was indicating that physico-sorption played a significant role in the biosorption of the phenol, 2-CPh, and 4-CPh onto MCNs.

3.6. Adsorption kinetics

The biosorption kinetics of phenol, 2-CPh, and 4-CPh onto MCNs were investigated by fitting the experimental data with two kinetic models, namely pseudo-first-order and pseudo-second-order. The pseudo-first-order equation and pseudo-second-order equation as expressed below (Eqs. (7) and (8)) [61,62]:

$$\ln(q_e - q_t) = \ln q_e - k_1 t \tag{7}$$

$$\frac{t}{q_t} = \frac{1}{k_2 q_e^2} + \left(\frac{1}{q_e}\right)t \tag{8}$$

Here q_t is the amount of phenol adsorbed at time t (mg/g), q_e is the amount of phenol adsorbed at equilibrium, k_1 is the adsorption rate constant (min^{-1}) for the first-order adsorption, and k_2 the pseudo-second-order rate constant. The rate constants k_1, k_2, and q_e were calculated from the slopes and intercepts of the linear plot of $\ln(q_e - q_t)$ or t/q_t against t respectively. A comparative statistical analysis of the linear first-order and second-order of adsorption rate constants, calculated q_e and R^2 values are given in the Table 3, for phenol, 2-CPh, and 4-CPh. As shown in Table 3, pseudo-second-order model is more valid for adsorption process than pseudo-first-order one [63].

3.7. Reusability

Desorption studies were conducted to analyze the possibility of reusing the adsorbent for further adsorption and to make the process more economical. After biosorption experiments the phenol, 2-CPh, and 4-CPh biosorbed MCNs were incubated with NaOH solution at pH 11.0 for 2 h at 30°C. To investigate the reusability of the adsorbent, for each period, the MCNs after desorption were separated with the help of a magnet

Table 3
Kinetic parameters of phenolic compounds on MCNs

	Pseudo-first-order				Pseudo-second-order		
	$q_{e,exp}$ (mg/g)	k_1 (min^{-1})	$q_{e,cal}$ (mg/g)	R^2	K_2 (g/mg/min)	$q_{e,cal}$ (mg/g)	R^2
Phenol							
100 ppm	96	0.493	47	0.938	0.030	99	0.999
150 ppm	110	0.279	42	0.746	0.039	108	0.999
200 ppm	130	0.332	58	0,993	0.040	130	0.999
2-chlorophenol							
100 ppm	106	0.323	38	0.883	0.221	107	0.999
150 ppm	129	0.330	52	0.997	0.033	133	0.998
200 ppm	146	0.318	54	0.913	0.024	147	0.999
4-chlorophenol							
100 ppm	127	0.380	56	0.996	0.208	127	0.999
150 ppm	136	0.540	51	0.993	0.052	139	0.999
200 ppm	160	0.330	57	0.998	0.028	162	0.999

and reused in adsorption experiments and the process was caried out for five times (see Fig. 8). The reduction in sorption percentages from the first to fiveth cycle was 17% for phenol, 28% for 2-CPh, and 24% for 4-CPh. As can be seen from Fig. 5, the decrease in the sorptin capacity of sorbent during the five soption trials might be due to the incompleted desorption of phenols at pH 11.0.

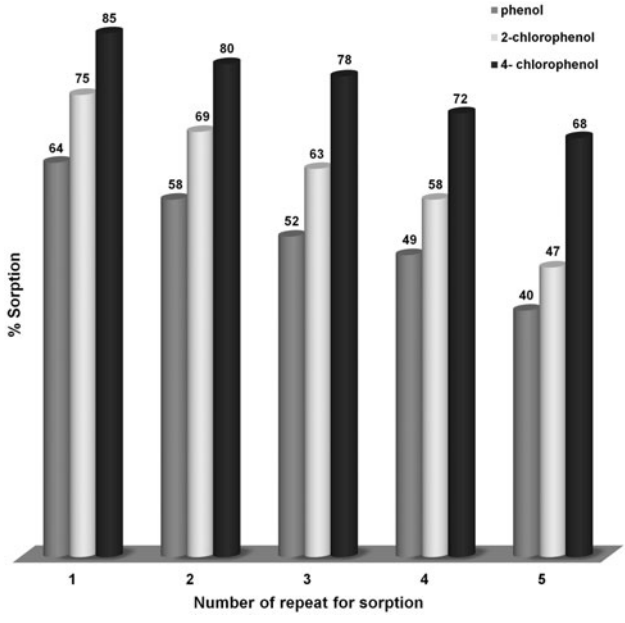

Fig. 8. Percent removal of phenol, 2-CPh, and 4-CPh on MCNs for repeated number of biosorption experiments.

4. Conclusions

In this study, the MCNs were proposed as a biosorbent for magnetic separation of phenol, 2-CPh, and 4-CPh from aqueous solutions and investigated the equilibrium and the dynamics of the adsorption. The size and biosorption properties of MCNs seemed reasonably convenient for the separation of the phenol, 2-CPh, and 4-CPh from aqueous solutions. The biosorption capacity of phenolic compounds onto the MCNs was depend on pH, contact time, the initial phenolic compounds concentration and adsorbent dose. High adsorption capacities were obtained in the pH range of 6.0–7.0 to remove the phenolic compounds. The adsorption capacity increased with increase in initial phenolic compounds concentration. Kinetic studies have shown that the reaction of adsorption is pseudo-second-order. The values of thermodynamic parameters obtained for the biosorption process indicated that the Freundlich isotherm model fitted quite well with the experimental data (correlation coefficient $R^2 \geq 0.98$), compared to the other two isotherm models.

In addition, the MCNs can be regenerated efficiently using NaOH solution at pH 11.0 because biosorption was the lowest at pH 11.0. The adsorbent was used for five repeated cycles for removal of the phenol, 2-CPh, and 4-CPh. The technique used in this study offered a convenient and efficient method for the preparation of the MCNs, which facilitated a more efficient biosorption of phenol, 2-CPh, and 4-CPh from aqueous solution and avoided secondary pollution of adsorbent to water.

Acknowledgments

This project is funded by the financial support from Dicle University Research Fund (DUBAP, Project No. 12-ZEF-110, 13-ZEF-28 and Project No. 13-ZEF-85).

References

[1] USEPA, List (phase 1) of hazardous constituents for ground-water monitoring: Final rule, Fed. Regist. 52 (1987) 25942–25953.
[2] O. Hamdaoui, E. Naffrechoux, Modeling of adsorption isotherms of phenol and chlorophenols onto granular activated carbon: Part I. Two-parameter models and equations allowing determination of thermodynamic parameters, J. Hazard. Mater. 147 (2007) 381–394.
[3] M. Ahmaruzzaman, Adsorption of phenolic compounds on low-cost adsorbents: A review, Adv. Colloid Interface Sci. 143 (2008) 48–67.
[4] M. Ahmaruzzaman, S.L. Gayatri, Activated neem leaf: A novel adsorbent for the removal of phenol, 4-nitrophenol, and 4-chlorophenol from aqueous solutions, J. Chem. Eng. Data 56 (2011) 3004–3016.
[5] M. Ahmaruzzaman, D.K. Sharma, Adsorption of phenols from wastewater, J. Colloid Interface Sci. 287 (2005) 14–24.
[6] G. Pigatto, A. Lodi, E. Finocchio, M.S.A. Palma, A. Converti, Chitin as biosorbent for phenol removal from aqueous solution: Equilibrium, kinetic and thermodynamic studies, Chem. Eng. Process. Process Intensif. 70 (2013) 131–139.
[7] J. Mittal, D. Jhare, H. Vardhan, A. Mittal, Utilization of bottom ash as a low-cost sorbent for the removal and recovery of a toxic halogen containing dye eosin yellow, Desalin. Water Treat. 52 (2013) 4508–4519.
[8] M. Ahmaruzzaman, V.K. Gupta, Rice husk and its ash as low-cost adsorbents in water and wastewater treatment, Ind. Eng. Chem. Res. 50 (2011) 13589–13613.
[9] H.-L. Jiang, J.-H. Tay, A.M. Maszenan, S.T.-L. Tay, Enhanced phenol biodegradation and aerobic granulation by two coaggregating bacterial strains, Environ. Sci. Technol. 40 (2006) 6137–6142.
[10] M. Djebbar, F. Djafri, M. Bouchekara, A. Djafri, Adsorption of phenol on natural clay, Appl. Water Sci. 2 (2012) 77–86.
[11] A. Rezaee, G.H. Pourtaghi, A. Khavanin, R.S. Mamoory, M. Ghaneian, H. Godini, Photocatalytic decomposition of gaseous toluene by TiO_2 nanoparticles coated on activated carbon, Iran. J. Environ. Health Sci. Eng. 5 (2008) 305–310.
[12] S. Tural, B. Tural, M.Ş. Ece, E. Yetkin, N. Özkan, Kinetic approach for the purification of nucleotides with magnetic separation, J. Sep. Sci. 37 (2014) 3370–3376.
[13] Y. Zou, Y. Chen, Z. Yan, C. Chen, J. Wang, S. Yao, Magnetic solid-phase extraction based on tetrabenzyl modified Fe_3O_4 nanoparticles for the analysis of trace polycyclic aromatic hydrocarbons in environmental water samples, The Analyst 138 (2013) 5904–5912.
[14] Y. Khollam, S. Dhage, H. Potdar, S. Deshpande, P. Bakare, S. Kulkarni, S. Date, Microwave hydrothermal preparation of submicron-sized spherical magnetite (Fe_3O_4) powders, Mater. Lett. 56 (2002) 571–577.
[15] A. Košak, D. Makovec, M. Drofenik, A. Žnidaršič, In situ synthesis of magnetic MnZn-ferrite nanoparticles using reverse microemulsions, J. Magn. Magn. Mater. 272–276 (2004) 1542–1544.
[16] C.-W. Chen, M.-Q. Chen, In situ synthesis and the catalytic properties of platinum colloids on polystyrene microspheres with surface-grafted poly (N-isopropylacrylamide), Chem. Commun. 7 (1998) 831–832.
[17] H. Lin, Y. Watanabe, M. Kimura, K. Hanabusa, H. Shirai, Preparation of magnetic poly (vinyl alcohol) (PVA) materials by *in situ* synthesis of magnetite in a PVA matrix, J. Appl. Polym. Sci. 87 (2003) 1239–1247.
[18] B. Tural, M. Kaya, N. Özkan, M. Volkan, Preparation and characterization of Ni-nitrilotriacetic acid bearing poly (methacrylic acid) coated superparamagnetic magnetite nanoparticles, J. Nanosci. Nanotechnol. 8 (2008) 695–701.
[19] A.-C. Chao, S.-S. Shyu, Y.-C. Lin, F.-L. Mi, Enzymatic grafting of carboxyl groups on to chitosan—To confer on chitosan the property of a cationic dye adsorbent, Bioresour. Technol. 91 (2004) 157–162.
[20] G. Crini, Non-conventional low-cost adsorbents for dye removal: A review, Bioresour. Technol. 97 (2006) 1061–1085.
[21] T. Saitoh, Y. Sugiura, K. Asano, M. Hiraide, Chitosan-conjugated thermo-responsive polymer for the rapid removal of phenol in water, React. Funct. Polym. 69 (2009) 792–796.
[22] S. Zheng, Z. Yang, Y.H. Park, Removal of chlorophenols from groundwater by chitosan sorption, Water Res. 38 (2004) 2315–2322.
[23] S.K. Nadavala, K. Swayampakula, V.M. Boddu, K. Abburi, Biosorption of phenol and o-chlorophenol from aqueous solutions on to chitosan–calcium alginate blended beads, J. Hazard. Mater. 162 (2009) 482–489.
[24] M.A.L. Milhome, D.D. Keukeleire, J.P. Ribeiro, R.F. Nascimento, T.V. Carvalho, D.C. Queiroz, Removal of phenol and conventional pollutants from aqueous effluent by chitosan and chitin, Quím. Nova 32 (2009) 2122–2127.
[25] N. Kumar, M. Suguna, M. Subbaiah, A. Reddy, N. Kumar, A. Krishnaiah, Adsorption of phenolic compounds from aqueous solutions onto chitosan-coated perlite beads as biosorbent, Ind. Eng. Chem. Res. 49 (2010) 9238–9247.
[26] J.-M. Li, X.-G. Meng, C.-W. Hu, J. Du, Adsorption of phenol, p-chlorophenol and p-nitrophenol onto functional chitosan, Bioresour. Technol. 100 (2009) 1168–1173.
[27] N. Siva Kumar, M. Venkata Subbaiah, A. Subba Reddy, A. Krishnaiah, Biosorption of phenolic compounds from aqueous solutions onto chitosan–abrus precatorius blended beads, J. Chem. Technol. Biotechnol. 84 (2009) 972–981.
[28] V.C. Srivastava, M.M. Swamy, I.D. Mall, B. Prasad, I.M. Mishra, Adsorptive removal of phenol by bagasse fly ash and activated carbon: Equilibrium, kinetics and thermodynamics, Colloids Surf. A 272 (2006) 89–104.
[29] B. Hameed, A. Rahman, Removal of phenol from aqueous solutions by adsorption onto activated carbon prepared from biomass material, J. Hazard. Mater. 160 (2008) 576–581.

[30] A. Kumar, S. Kumar, s. Kumar, D.V. Gupta, Adsorption of phenol and 4-nitrophenol on granular activated carbon in basal salt medium: Equilibrium and kinetics, J. Hazard. Mater. 147 (2007) 155–166.
[31] B. Özkaya, Adsorption and desorption of phenol on activated carbon and a comparison of isotherm models, J. Hazard. Mater. 129 (2006) 158–163.
[32] S. Al-Asheh, F. Banat, L. Abu-Aitah, Adsorption of phenol using different types of activated bentonites, Sep. Purif. Technol. 33 (2003) 1–10.
[33] A.T. Mohd, B.H. Din, A.L. Hameed, Ahmad, Batch adsorption of phenol onto physiochemical-activated coconut shell, J. Hazard. Mater. 161 (2009) 1522–1529.
[34] B.K. Singh, N.S. Rawat, Comparative sorption equilibrium studies of toxic phenols on flyash and impregnated flyash, J. Chem. Technol. Biotechnol. 61 (1994) 307–317.
[35] M. Akçay, G. Akçay, The removal of phenolic compounds from aqueous solutions by organophilic bentonite, J. Hazard. Mater. 113 (2004) 189–193.
[36] B. Koumanova, P. Peeva-Antova, Adsorption of p-chlorophenol from aqueous solutions on bentonite and perlite, J. Hazard. Mater. 90 (2002) 229–234.
[37] B. Tural, İ. Şimşek, S. Tural, B. Çelebi, A.S. Demir, Carboligation reactivity of benzaldehyde lyase (BAL, EC 4.1. 2.38) covalently attached to magnetic nanoparticles, Tetrahedron: Asymmetry 24 (2013) 260–268.
[38] B. Tural, S. Tural, E. Ertaş, İ. Yalınkılıç, A.S. Demir, Purification and covalent immobilization of benzaldehyde lyase with heterofunctional chelate-epoxy modified magnetic nanoparticles and its carboligation reactivity, J. Mol. Catal. B Enzym. 95 (2013) 41–47.
[39] Y. Kawamura, H. Yoshida, S. Asai, I. Kurahashi, H. Tanibe, Effects of chitosan concentration and precipitation bath concentration on the material properties of porous crosslinked chitosan beads, Sep. Sci. Technol. 32 (1997) 1959–1974.
[40] G.-Y. Li, Y.-R. Jiang, K.-L. Huang, P. Ding, J. Chen, Preparation and properties of magnetic Fe_3O_4–chitosan nanoparticles, J. Alloys Compd. 466 (2008) 451–456.
[41] Y. Wu, J. Guo, W. Yang, C. Wang, S. Fu, Preparation and characterization of chitosan–poly(acrylic acid) polymer magnetic microspheres, Polymer 47 (2006) 5287–5294.
[42] M. Yamaura, R. Camilo, L. Sampaio, M. Macêdo, M. Nakamura, H. Toma, Preparation and characterization of (3-aminopropyl) triethoxysilane-coated magnetite nanoparticles, J. Magn. Magn. Mater. 279 (2004) 210–217.
[43] C. Yuwei, W. Jianlong, Preparation and characterization of magnetic chitosan nanoparticles and its application for Cu(II) removal, Chem. Eng. J. 168 (2011) 286–292.
[44] Y. Osuna, K.M. Gregorio-Jauregui, J.G. Gaona-Lozano, I.M. de la Garza-Rodríguez, A. Ilyna, E.D. Barriga-Castro, H. Saade, R.G. López, Chitosan-coated magnetic nanoparticles with low chitosan content prepared in one-step, J. Nanomater. 2012 (2012) 1–7.
[45] L. Zang, J. Qiu, X. Wu, W. Zhang, E. Sakai, Y. Wei, Preparation of magnetic chitosan nanoparticles as support for cellulase ımmobilization, Ind. Eng. Chem. Res. 53 (2014) 3448–3454.
[46] L. Zhu, B. Chen, X. Shen, Sorption of phenol, p-nitrophenol, and aniline to dual-cation organobentonites from water, Environ. Sci. Technol. 34 (2000) 468–475.
[47] Z. Rawajfih, N. Nsour, Characteristics of phenol and chlorinated phenols sorption onto surfactant-modified bentonite, J. Colloid Interface Sci. 298 (2006) 39–49.
[48] G. Mihoc, R. Ianoş, C. Păcurariu, Adsorption of phenol and p-chlorophenol from aqueous solutions by magnetic nanopowder, Water Sci. Technol. 69 (2014) 385–391.
[49] I. Langmuir, The adsorptıon of gases on plane surfaces of glass, mica and platınum, J. Am. Chem. Soc. 40 (1918) 1361–1403.
[50] A. Mittal, Removal of the dye, Amaranth from waste water using hen feathers as potential adsorbent, Electron. J. Environ. Agric. Food Chem. 5 (2006) 1296–1305.
[51] H. Freundlich, Über die adsorption in Lösungen, Z. Phys. Chem. (Leipzig) 57 (1906) 385–470.
[52] P. SenthilKumar, S. Ramalingam, R. Abhinaya, S.D. Kirupha, T. Vidhyadevi, S. Sivanesan, Adsorption equilibrium, thermodynamics, kinetics, mechanism and process design of zinc(II) ions onto cashew nut shell, Can. J. Chem. Eng. 90 (2012) 973–982.
[53] D.G. Kinniburgh, General purpose adsorption isotherms, Environ. Sci. Technol. 20 (1986) 895–904.
[54] M. Özacar, I.A. Şengil, Adsorption of reactive dyes on calcined alunite from aqueous solutions, J. Hazard. Mater. 98 (2003) 211–224.
[55] M. Dubinin, The potential theory of adsorption of gases and vapors for adsorbents with energetically nonuniform surfaces, Chem. Rev. 60 (1960) 235–241.
[56] M. Dubinin, Modern state of the theory of volume filling of micropore adsorbents during adsorption of gases and steams on carbon adsorbents, Zh. Fiz. Khim. 39 (1965) 1305–1317.
[57] M. Dubinin, L. Radushkevich, Equation of the characteristic curve of activated charcoal, Chem. Zentralbl. 1 (1947) 875–890.
[58] S.J. Gregg, K.S.W. Sing, Adsorption, Surface Area, and Porosity, Academic Press, London, 1967.
[59] A. Benhammou, A. Yaacoubi, L. Nibou, B. Tanouti, Adsorption of metal ions onto moroccan stevensite: Kinetic and isotherm studies, J. Colloid Interface Sci. 282 (2005) 320–326.
[60] Z. Hongxia, W. Chuanxi, T. Zuyi, W. Wangsuo, Effects of nitrate, fulvate, phosphate, phthalate, salicylate and catechol on the sorption of uranyl onto SiO_2: A comparative study, J. Radioanal. Nucl. Chem. 287 (2011) 13–20.
[61] M.J. Ahmed, S.K. Dhedan, Equilibrium isotherms and kinetics modeling of methylene blue adsorption on agricultural wastes-based activated carbons, Fluid Phase Equilib. 317 (2012) 9–14.
[62] R.N. Goyal, A. Kumar, A. Mittal, Oxidation chemistry of adenine and hydroxyadenines at pyrolytic graphite electrodes, J. Chem. Soc. Perkin Trans. 2 2 (1991) 1369–1375.
[63] K.Z. Elwakeel, Removal of reactive black 5 from aqueous solutions using magnetic chitosan resins, J. Hazard. Mater. 167 (2009) 383–392.